ADP-22-27/T1198, DESY-22-145, LTH 1307

Moments and power corrections of longitudinal and transverse proton structure functions from lattice QCD

M. Batelaan,[1] K. U. Can,[1] A. Hannaford-Gunn,[1] R. Horsley,[2] Y. Nakamura,[3] H. Perlt,[4] P. E. L. Rakow,[5] G. Schierholz,[6] H. Stüben,[7] R. D. Young,[1] and J. M. Zanotti[1]

(QCDSF/UKQCD/CSSM Collaborations)

[1] *CSSM, Department of Physics, The University of Adelaide, Adelaide SA 5005, Australia*
[2] *School of Physics and Astronomy, University of Edinburgh, Edinburgh EH9 3JZ, UK*
[3] *RIKEN Center for Computational Science, Kobe, Hyogo 650-0047, Japan*
[4] *Institut für Theoretische Physik, Universität Leipzig, 04103 Leipzig, Germany*
[5] *Theoretical Physics Division, Department of Mathematical Sciences, University of Liverpool, Liverpool L69 3BX, United Kingdom*
[6] *Deutsches Elektronen-Synchrotron DESY, Notkestr. 85, 22607 Hamburg, Germany.*
[7] *Regionales Rechenzentrum, Universität Hamburg, 20146 Hamburg, Germany*

We present a simultaneous extraction of the moments of F_2 and F_L structure functions of the proton at a range of photon virtuality, Q^2. This is achieved by computing the forward Compton amplitude via an application of the second-order Feynman-Hellmann method. We find the moments of $F_{2,L}$ in good agreement with experimental values. By studying the Q^2 dependence of F_2 moments, we estimate the power corrections.

Keywords: nucleon structure, parton distributions, Feynman Hellmann, Compton amplitude, transverse, longitudinal, structure functions, power corrections, scaling, lattice QCD

Introduction.— Nucleon structure functions are encoded by the differential cross sections for inclusive electron–proton scattering. In terms of the partonic structure of the nucleon, the deep inelastic cross sections are dominated by the transverse structure function, F_2, which hence provides the primary constraint on the parton distributions. On the other hand, the longitudinal structure function, F_L, provides important information on the QCD structure of the proton. With a perturbatively small and calculable leading-twist component [1], F_L offers a direct measure of higher-twist effects [2]. It also offers sensitivity to the low-x gluon distribution [3].

Although the small nature of the longitudinal structure function makes it more challenging to isolate, measurements by HERA [4] and Jefferson Lab [5, 6] have enabled a direct extraction of several low moments of F_L across a range of Q^2 [7]. The results reveal a tension with global PDF fits [8–10] at lower Q^2 that might indicate non-negligible higher-twist effects or an increased high-x gluon distribution [7]. It is therefore highly desirable to be able to provide first-principles theoretical predictions regarding F_L, preferably at intermediate Q^2 values where the non-perturbative effects become significant. Furthermore, an improved theoretical constraint on power corrections in the structure functions generally could be particularly beneficial in global PDF analyses.

Lattice QCD simulations of the structure functions conventionally utilise the operator product expansion (OPE) approach. Lattice simulations have been successful in computing the twist-2 contributions, however the higher-twist terms mix with those of lower-twist which gives rise to complications in the renormalisation procedure [11]. This setback has limited lattice QCD to investigations of the leading-twist contributions [12, 13], with fewer works on twist-3 contributions [14–16].

In this Letter, we present a simultaneous extraction of the low moments of the nucleon structure functions F_2 and F_L from the forward Compton amplitude calculated on the lattice. This approach circumvents the operator mixing issues since the amplitude accounts for the mixing and renormalisation and contains all twist contributions. Previous successful calculations of the Compton amplitude, leading to a determination of the moments of the nucleon structure function F_1, have been reported in [17, 18], and recently extended to off-forward kinematics [19].

Compton amplitude and moments of structure functions.— In order to access the structure functions, we consider the unpolarised forward Compton tensor,

$$T_{\mu\nu}(p,q) = \left(-g_{\mu\nu} + \frac{q_\mu q_\nu}{q^2}\right)\mathcal{F}_1(\omega,Q^2) + \frac{\hat{P}_\mu \hat{P}_\nu}{p\cdot q}\mathcal{F}_2(\omega,Q^2), \tag{1}$$

where q (p) is the momentum of the virtual photon (nucleon), $\hat{P}_\mu \equiv p_\mu - (p\cdot q)q_\mu/q^2$, $\omega = (2p\cdot q)/Q^2$ and $Q^2 = -q^2$. The Lorentz invariant Compton structure functions $\mathcal{F}_{1,2}$ are related to the physical structure functions $F_{1,2}$ via the optical theorem, $\operatorname{Im}\mathcal{F}_{1,2}(\omega,Q^2) = 2\pi F_{1,2}(x,Q^2)$. Making use of analyticity, crossing symmetry, and the optical theorem, the Compton structure functions satisfy the familiar dispersion relations [20],

$$\overline{\mathcal{F}}_1(\omega,Q^2) = 2\omega^2 \int_0^1 dx \frac{2x\,F_1(x,Q^2)}{1-x^2\omega^2 - i\epsilon}, \tag{2}$$

$$\mathcal{F}_2(\omega,Q^2) = 4\omega \int_0^1 dx\, \frac{F_2(x,Q^2)}{1-x^2\omega^2 - i\epsilon}, \tag{3}$$

where $\overline{\mathcal{F}}_1(\omega,Q^2) = \mathcal{F}_1(\omega,Q^2) - \mathcal{F}_1(0,Q^2)$.

The parametrisation of the forward Compton amplitude in terms of F_1 and F_2 is not unique. Alternatively, we can consider a parametrisation in terms of the transverse, $2xF_1$, and longitudinal, F_L, structure functions [20–23]. The latter is given by [20, 22],

$$F_L(x,Q^2) = \left(1 - \frac{4M_N^2}{Q^2}x^2\right) F_2(x,Q^2) - 2xF_1(x,Q^2), \quad (4)$$

which can directly be obtained from the ratio of cross sections [22, 23]. Here M_N is the mass of the nucleon. As $Q^2 \to \infty$, Eq. (4) reduces to $F_L(x) \to F_2(x) - 2xF_1(x)$, which vanishes in the quark-parton model due to the familiar Callan-Gross relation. In QCD, F_L is $\mathcal{O}(\alpha_s)$ suppressed at leading twist and any power correction may be identified as higher twist.

Writing,

$$\mathcal{F}_L(\omega,Q^2) = -\mathcal{F}_1(\omega,Q^2) + \left(\frac{\omega}{2} + \frac{2M_N^2}{\omega Q^2}\right)\mathcal{F}_2(\omega,Q^2), \quad (5)$$

we can express $\overline{\mathcal{F}}_L$ by a subtracted dispersion relation in terms of F_L,

$$\begin{aligned}\overline{\mathcal{F}}_L(\omega,Q^2) = \frac{8M_N^2}{Q^2}\int_0^1 dx F_2(x,Q^2) \\ + 2\omega^2 \int_0^1 dx \frac{F_L(x,Q^2)}{1 - x^2\omega^2 - i\epsilon},\end{aligned} \quad (6)$$

where $\overline{\mathcal{F}}_L(\omega,Q^2) = \mathcal{F}_L(\omega,Q^2) + \mathcal{F}_1(0,Q^2)$.

Expanding the integrands in Eqs. (2), (3) and (6) as a geometric series, we express the Compton structure functions as infinite sums over the Mellin moments of the inelastic structure functions,

$$\overline{\mathcal{F}}_{1,L}(\omega,Q^2) = \sum_{n=0}^{\infty} 2\omega^{2n} M_{2n}^{(1,L)}(Q^2), \quad (7)$$

$$\mathcal{F}_2(\omega,Q^2) = \sum_{n=1}^{\infty} 4\omega^{2n-1} M_{2n}^{(2)}(Q^2), \quad (8)$$

where $M_0^{(1)}(Q^2) = 0$, $2M_0^{(L)}(Q^2) = \frac{8M_N^2}{Q^2} M_2^{(2)}(Q^2)$,

$$M_{2n}^{(1)}(Q^2) = 2\int_0^1 dx\, x^{2n-1} F_1(x,Q^2), \quad (9)$$

$$M_{2n}^{(2,L)}(Q^2) = \int_0^1 dx\, x^{2n-2} F_{2,L}(x,Q^2), \quad (10)$$

for $n > 0$.

For our purposes, it is convenient to express the expansion of $\mathcal{F}_2$ in terms of the independently positive definite moments of F_1 and F_L,

$$\frac{\mathcal{F}_2(\omega)}{\omega} = \frac{\tau}{(1+\tau\omega^2)} \sum_{n=0}^{\infty} 4\omega^{2n}\left[M_{2n}^{(1)} + M_{2n}^{(L)}\right], \quad (11)$$

where $\tau = Q^2/4M_N^2$. The intercept at $\omega = 0$ is proportional to the lowest moment of F_2, i.e. $M_2^{(2)}(Q^2)$. Higher moments are given by the appropriate combinations of the moments of F_1 and F_L.

In the following discussion, we provide the details of our procedure for extracting the moments directly from the Compton amplitude obtained in a lattice simulation.

The Feynman-Hellmann approach.— The novel idea is to compute the Compton amplitude by means of the second-order Feynman-Hellmann theorem as derived and described in detail in [18]. Here we summarise the procedure relevant to this work. We perturb the fermion action by the renormalised local vector current,

$$S(\lambda) = S + \lambda \int d^3z (e^{i\mathbf{q}\cdot\mathbf{z}} + e^{-i\mathbf{q}\cdot\mathbf{z}})\mathcal{J}_\mu(z). \quad (12)$$

The perturbation is introduced on the valence quarks only, hence only quark-line connected contributions are taken into account in this work. For the perturbation of valence and sea quarks see [24].

We consider $q_3 = p_3 = 0$ and current components $\mathcal{J}_0$ and $\mathcal{J}_3$, enabling us to compute T_{00} and T_{33}. These are then given by the second order energy shift [18],

$$\left.\frac{\partial^2 E_{N_\lambda}(\mathbf{p})}{\partial\lambda^2}\right|_{\lambda=0} = -\frac{T_{\mu\mu}(p,q) + T_{\mu\mu}(p,-q)}{2E_N(\mathbf{p})}, \quad (13)$$

where $T_{\mu\nu}$ is the Compton tensor defined in Eq. (1), $q = (0,\mathbf{q})$ is the external momentum encoded by Eq. (12), and $E_{N_\lambda}(\mathbf{p})$ is the nucleon energy at momentum $\mathbf{p}$ in the presence of a background field of strength λ. This expression is the principal relation that we use to access the Compton amplitude and hence the Compton structure functions as described below.

Simulation and analysis.—Our lattice simulations are carried out on QCDSF/UKQCD-generated 2 + 1-flavour gauge configurations. We utilise two ensembles with volumes $V = [32^3 \times 64, 48^3 \times 96]$, and couplings $\beta = [5.50, 5.65]$ corresponding to lattice spacings $a = [0.074(2), 0.068(3)]$ fm respectively. The quark masses are tuned to the $SU(3)$ symmetric point where the masses of all three quark flavours are set to approximately the physical flavour-singlet mass, $\overline{m} = (2m_s + m_l)/3$ [25, 26], yielding $m_\pi \approx [470, 420]$MeV. The calculations are done for several values of $\mathbf{q}$. Multiple values of ω are accessed by varying the nucleon momentum $\mathbf{p}$.

By attaching the current selectively to the u and d quarks, respectively, we obtain the flavour diagonal contributions uu and dd corresponding to a handbag diagram at leading twist, and the mixed-flavour piece, ud, which is purely higher-twist, corresponding to a cat's ears diagram [27]. We typically compute the energy shifts, $\Delta E_{\mathbf{p},N_\lambda}$, for two λ values (see Ref. [18]) and perform polynomial fits of the form, $\Delta E_{\mathbf{p},N_\lambda} = \lambda^2 \left.\frac{\partial^2 E_{N_\lambda}(\mathbf{p})}{\partial\lambda^2}\right|_{\lambda=\mathbf{0}} + \mathcal{O}(\lambda^4)$, to determine the Compton amplitude. Choosing $\lambda = \mathcal{O}(10^{-2})$, higher order $\mathcal{O}(\lambda^4)$ terms are heavily suppressed.

The ω dependence of the Compton structure functions is mapped by extracting the amplitude for each pair of $(\mathbf{q},\mathbf{p})$. Subsequently, extraction of the moments from the Compton structure functions follows the methodology described in [18]. A simultaneous fit of $\overline{\mathcal{F}}_1$ (Eq. (7)) and $\mathcal{F}_2/\omega$ (Eq. (11)) is performed in a Bayesian framework to determine the first few Mellin moments of the structure functions. We truncate both series at $n = 4$ (inclusive) when determining the moments. These moments are enforced to be positive definite and monotonically decreasing. Note that the positivity bound does not hold for the ud contributions but they are constrained by $\left|M_{2n}^{ud}(Q^2)\right|^2 \leq 4M_{2n}^{uu}(Q^2)M_{2n}^{dd}(Q^2)$, since the total inclusive cross section (hence each moment) is positive for any value of the quark charges and at all kinematics. The sequences of individual uu, dd or ud moments are selected according to the standard probability distribution, where the diagonal of the full covariance matrix is used in the χ^2 function. We account for the correlations between the data points by doing a bootstrap analysis.

Results.— We show the ω dependence of the Compton structure functions along with their fit curves in Fig. 1 for a representative case of $Q^2 = 4.86\,\mathrm{GeV}^2$ calculated on the $48^3 \times 96$ ensemble. We keep terms up to $\mathcal{O}(w^8)$ in the fit polynomials Eqs. (7) and (11). The lowest two moments are insensitive to the addition of higher order terms.

The lowest moments of the structure functions $F_{2,L}$ obtained from the $32^3 \times 64$ and $48^3 \times 96$ ensembles are shown in Figures 2 and 3 as a function of Q^2 for the proton. Note that the moments of the proton are constructed via $M_{2,p}^{(2,L)} = \frac{4}{9}M_{2,uu}^{(2,L)} + \frac{1}{9}M_{2,dd}^{(2,L)} - \frac{2}{9}M_{2,ud}^{(2,L)}$. Our F_2 moments are in remarkable agreement with the experimental moments [28].

Since the Compton amplitude includes all power corrections, we can estimate the leading power correction (i.e. twist-4) by studying the Q^2 behaviour of the moments. Higher-twist contributions are suppressed by powers of $1/Q^2$ so one expects to have sizeable contributions for intermediate to low Q^2. Their effect (at the lowest order) can be modelled by the twist expansion,

$$M_{2,h}^{(2)}(Q^2) = M_{2,h}^{(2)} + C_{2,h}^{(2)}/Q^2 + \mathcal{O}(1/Q^4), \qquad (14)$$

where $h \in \{uu, dd, p\}$. We utilise only the $M_2^{(2)}(Q^2)$ moments obtained on the $48^3 \times 96$ ensemble to study the power corrections. We show our fit (Eq. (14)) in Fig. 2. The extracted values for $M_{2,h}^{(2)}$ and $C_{2,h}^{(2)}$ are collected in Table I. We note that our results could be useful for studies investigating the power corrections in the language of infrared renormalons [29–31].

We compare the lowest (Cornwall-Norton) moment of F_L to the experimentally determined Nachtmann moments [7] in Fig. 3. While we are unable to resolve a definitive signal for the F_L moments, we are able to set

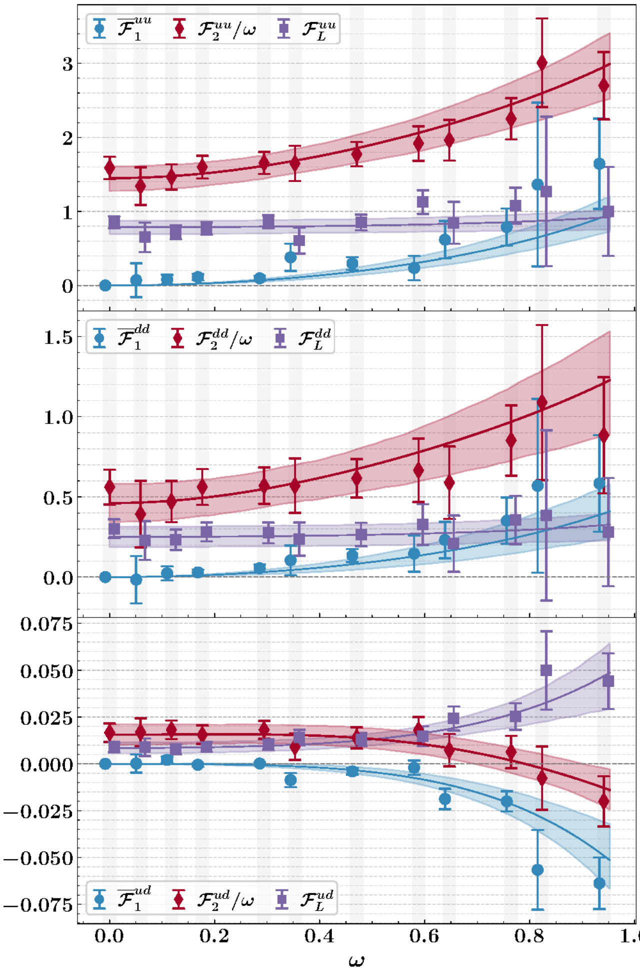

Figure 1. ω dependence of the Compton structure functions $\overline{\mathcal{F}}_1$, $\mathcal{F}_2$, and $\overline{\mathcal{F}}_L$ at $Q^2 = 4.86\,\mathrm{GeV}^2$. We show the uu (top), dd (middle) and ud (bottom) contributions. Coloured shaded bands show the fits with their 68% credible region of the highest posterior density. Points are displaced for clarity.

Table I. Extracted asymptotic values of the moments and the coefficients of the power correction terms. The power corrections are quoted at the scale of the nucleon mass $Q^2 = M_N^2$.

h	$M_{2,h}^{(2)}$	$C_{2,h}^{(2)}/M_N^2$
uu	0.268(13)	0.206(24)
dd	0.146(7)	0.024(14)
p	0.135(6)	0.091(11)

an upper bound that is compatible with the experimental moments.

It is interesting to compare $M_2^{(L)}$ determined from the relation [1],

$$M_{2,p}^{(L),\mathrm{twist-2}}(Q^2) = \frac{4}{9\pi}\alpha_s(Q^2)M_{2,p}^{(2),\mathrm{twist-2}}(Q^2), \qquad (15)$$

where we replace the leading-twist moment on RHS with

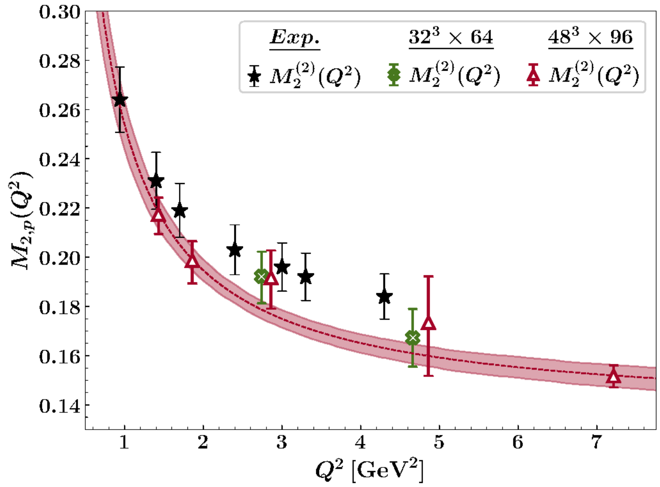

Figure 2. Q^2 dependence of the lowest moments of F_2 for the proton. Filled stars are the experimental Cornwall-Norton moments of F_2 [28]. Red band is the fit (Eq. (14)) to the $48^3 \times 96$ data points.

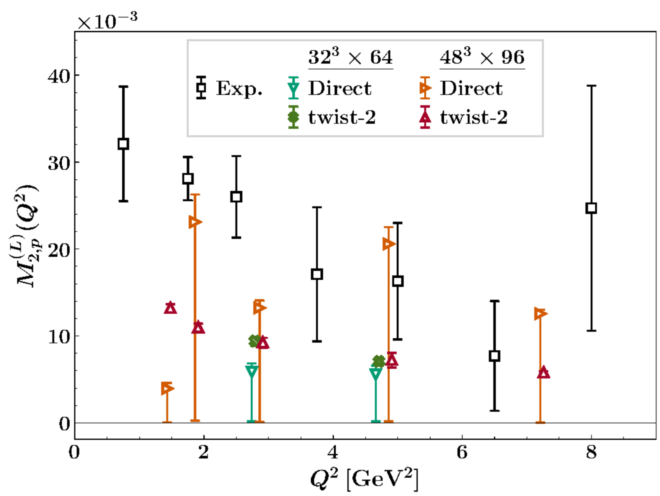

Figure 3. Lowest moment of the proton's longitudinal structure function $M_{2,p}^{(L)}$ as a function of Q^2. We compare our results (Direct) to the experimental Nachtmann moments (open black squares) taken from [7]. Asymmetric error bars indicate that our posterior distributions are highly skewed (non-Gaussian). We also show the moments (twist-2) determined via the relation, Eq. (15), using our determination of $M_{2,p}^{(2)}$ from the current work. Twist-2 points are displaced for clarity.

$M_{2,p}^{(2)}(Q^2)$ from the current work as an approximation. We use the value of $\alpha_s(Q^2)$ at $\mu = Q^2$ at the four-loop order by running its value from the $\mu_0 = M_\tau$ scale with $n_f = 3$ active flavours using the `CRunDec` package [32, 33].

The Q^2 behaviour is in good agreement with experimental points as shown in Fig. 3. With improved precision in future studies, contrasting the direct determination and twist-2 part of the lowest few moments of F_L would provide improved constraints on higher-twist effects.

Conclusions.— We have presented a simultaneous extraction of the lowest moments of the proton structure functions $F_{2,L}$. A first look into the moments of F_L is given. This has been possible in a lattice QCD setting for the first time thanks to our recent advances in calculating the forward Compton amplitude via an application of the second-order Feynman-Hellmann theorem.

Already at unphysical quark masses, we find good agreement with the moments determined from experiments. Our investigations solidify the versatility of the Compton amplitude approach and pave the way for reliable and systematically improvable first-principles studies of the structure functions and power corrections, complementing the experiments and other lattice or non-lattice methods.

Acknowledgments.— We would like to thank Wally Melnitchouk for fruitful discussions. The numerical configuration generation (using the BQCD lattice QCD program [34])) and data analysis (using the Chroma software library [35]) was carried out on the DiRAC Blue Gene Q and Extreme Scaling (EPCC, Edinburgh, UK) and Data Intensive (Cambridge, UK) services, the GCS supercomputers JUQUEEN and JUWELS (NIC, Jülich, Germany) and resources provided by HLRN (The North-German Supercomputer Alliance), the NCI National Facility in Canberra, Australia (supported by the Australian Commonwealth Government) and the Phoenix HPC service (University of Adelaide). RH is supported by STFC through grant ST/P000630/1. PELR is supported in part by the STFC under contract ST/G00062X/1. KUC, RDY and JMZ are supported by the Australian Research Council grants DP190100297 and DP220103098. For the purpose of open access, the authors have applied a Creative Commons Attribution (CC BY) licence to any Author Accepted Manuscript version arising from this submission.

[1] G. Altarelli and G. Martinelli, Transverse momentum of jets in electroproduction from quantum chromodynamics, Physics Letters B **76**, 89 (1978).
[2] S. Choi, T. Hatsuda, Y. Koike, and S. H. Lee, Twist four matrix elements of the nucleon from recent DIS data at CERN and SLAC, Phys. Lett. B **312**, 351 (1993), arXiv:hep-ph/9303272.
[3] A. M. Cooper-Sarkar, G. Ingelman, K. R. Long, R. G. Roberts, and D. H. Saxon, Measurement of the Longitudinal Structure Function and the Small X Gluon Density of the Proton, Z. Phys. C **39**, 281 (1988).
[4] F. D. Aaron *et al.* (H1 Collaboration), Measurement of the Inclusive e\pmp Scattering Cross Section at High Inelasticity y and of the Structure Function F_L, Eur. Phys. J. C **71**, 1579 (2011), arXiv:1012.4355 [hep-ex].

[5] Y. Liang *et al.* (Jefferson Lab Hall C E94-110 Collaboration), Measurement of R = sigma(L) / sigma(T) and the separated longitudinal and transverse structure functions in the nucleon resonance region, (2004), arXiv:nucl-ex/0410027.

[6] https://hallcweb.jlab.org/resdata/.

[7] P. Monaghan, A. Accardi, M. E. Christy, C. E. Keppel, W. Melnitchouk, and L. Zhu, Moments of the longitudinal proton structure function F_L from global data in the Q^2 range 0.75-45.0 $(\mathrm{GeV}/c)^2$, Phys. Rev. Lett. **110**, 152002 (2013), arXiv:1209.4542 [nucl-ex].

[8] A. Accardi, W. Melnitchouk, J. F. Owens, M. E. Christy, C. E. Keppel, L. Zhu, and J. G. Morfin, Uncertainties in determining parton distributions at large x, Phys. Rev. D **84**, 014008 (2011), arXiv:1102.3686 [hep-ph].

[9] S. Alekhin, J. Blumlein, S. Klein, and S. Moch, The 3, 4, and 5-flavor NNLO Parton from Deep-Inelastic-Scattering Data and at Hadron Colliders, Phys. Rev. D **81**, 014032 (2010), arXiv:0908.2766 [hep-ph].

[10] A. D. Martin, W. J. Stirling, R. S. Thorne, and G. Watt, Parton distributions for the LHC, Eur. Phys. J. C **63**, 189 (2009), arXiv:0901.0002 [hep-ph].

[11] G. Martinelli and C. T. Sachrajda, On the difficulty of computing higher twist corrections, Nucl. Phys. B **478**, 660 (1996), arXiv:hep-ph/9605336.

[12] H.-W. Lin *et al.*, Parton distributions and lattice QCD calculations: A community white paper, Progress in Particle and Nuclear Physics **100**, 107 (2018).

[13] M. Constantinou *et al.*, Lattice QCD Calculations of Parton Physics, (2022), arXiv:2202.07193 [hep-lat].

[14] M. Gockeler, R. Horsley, D. Pleiter, P. E. L. Rakow, A. Schafer, G. Schierholz, H. Stuben, and J. M. Zanotti, Investigation of the second moment of the nucleon's g(1) and g(2) structure functions in two-flavor lattice QCD, Phys. Rev. D **72**, 054507 (2005), arXiv:hep-lat/0506017.

[15] S. Bhattacharya, K. Cichy, M. Constantinou, A. Metz, A. Scapellato, and F. Steffens, Insights on proton structure from lattice QCD: The twist-3 parton distribution function $g_T(x)$, Phys. Rev. D **102**, 111501 (2020), arXiv:2004.04130 [hep-lat].

[16] S. Bhattacharya, K. Cichy, M. Constantinou, A. Metz, A. Scapellato, and F. Steffens, Parton distribution functions beyond leading twist from lattice QCD: The hL(x) case, Phys. Rev. D **104**, 114510 (2021), arXiv:2107.02574 [hep-lat].

[17] A. J. Chambers, R. Horsley, Y. Nakamura, H. Perlt, P. E. L. Rakow, G. Schierholz, A. Schiller, K. Y. Somfleth, R. D. Young, and J. M. Zanotti (QCDSF Collaboration), Nucleon Structure Functions from Operator Product Expansion on the Lattice, Phys. Rev. Lett. **118**, 242001 (2017), arXiv:1703.01153 [hep-lat].

[18] K. U. Can, A. Hannaford-Gunn, R. Horsley, Y. Nakamura, H. Perlt, P. E. L. Rakow, G. Schierholz, K. Y. Somfleth, H. Stüben, R. D. Young, and J. M. Zanotti (QCDSF/UKQCD/CSSM Collaborations), Lattice QCD evaluation of the Compton amplitude employing the Feynman-Hellmann theorem, Phys. Rev. D **102**, 114505 (2020), arXiv:2007.01523 [hep-lat].

[19] A. Hannaford-Gunn, K. U. Can, R. Horsley, Y. Nakamura, H. Perlt, P. E. L. Rakow, H. Stüben, G. Schierholz, R. D. Young, and J. M. Zanotti (CSSM/QCDSF/UKQCD), Generalized parton distributions from the off-forward Compton amplitude in lattice QCD, Phys. Rev. D **105**, 014502 (2022), arXiv:2110.11532 [hep-lat].

[20] D. Drechsel, B. Pasquini, and M. Vanderhaeghen, Dispersion relations in real and virtual Compton scattering, Phys. Rept. **378**, 99 (2003), arXiv:hep-ph/0212124.

[21] L. N. Hand, Experimental investigation of pion electroproduction, Phys. Rev. **129**, 1834 (1963).

[22] A. Bodek *et al.*, Experimental Studies of the Neutron and Proton Electromagnetic Structure Functions, Phys. Rev. D **20**, 1471 (1979).

[23] W. Melnitchouk, R. Ent, and C. Keppel, Quark-hadron duality in electron scattering, Phys. Rept. **406**, 127 (2005), arXiv:hep-ph/0501217.

[24] A. Chambers, R. Horsley, Y. Nakamura, H. Perlt, D. Pleiter, P. E. L. Rakow, G. Schierholz, A. Schiller, H. Stüben, R. D. Young, and J. M. Zanotti, Disconnected contributions to the spin of the nucleon, Phys. Rev. D **92**, 114517 (2015), arXiv:1508.06856 [hep-lat].

[25] W. Bietenholz, V. Bornyakov, N. Cundy, M. Göckeler, R. Horsley, A. D. Kennedy, W. G. Lockhart, Y. Nakamura, H. Perlt, D. Pleiter, P. E. L. Rakow, A. Schäfer, G. Schierholz, A. Schiller, H. Stüben, and J. M. Zanotti (QCDSF-UKQCD Collaboration), Tuning the strange quark mass in lattice simulations, Phys. Lett. **B690**, 436 (2010), arXiv:1003.1114 [hep-lat].

[26] W. Bietenholz, M. Bornyakov, V. Göckeler, R. Horsley, W. G. Lockhart, Y. Nakamura, H. Perlt, D. Pleiter, P. E. L. Rakow, G. Schierholz, A. Schiller, T. Streuer, H. Stüben, F. Winter, and J. M. Zanotti (QCDSF-UKQCD Collaboration), Flavour blindness and patterns of flavour symmetry breaking in lattice simulations of up, down and strange quarks, Phys. Rev. D **84**, 054509 (2011), arXiv:1102.5300 [hep-lat].

[27] Note that we are mentioning the leading-twist diagrams for the clarity of the discussion. In reality, the Compton amplitude includes all twist contributions.

[28] C. S. Armstrong, R. Ent, C. E. Keppel, S. Liuti, G. Niculescu, and I. Niculescu, Moments of the proton F(2) structure function at low Q**2, Phys. Rev. D **63**, 094008 (2001), arXiv:hep-ph/0104055.

[29] E. Stein, M. Meyer-Hermann, L. Mankiewicz, and A. Schafer, IR Renormalon contribution to the longitudinal structure function F(L), Phys. Lett. B **376**, 177 (1996), arXiv:hep-ph/9601356.

[30] M. Dasgupta and B. R. Webber, Power corrections and renormalons in deep inelastic structure functions, Phys. Lett. B **382**, 273 (1996), arXiv:hep-ph/9604388.

[31] M. Beneke and V. M. Braun, Renormalons and power corrections, At The Frontier of Particle Physics , 1719 (2000), arXiv:hep-ph/0010208.

[32] K. G. Chetyrkin, J. H. Kuhn, and M. Steinhauser, RunDec: A Mathematica package for running and decoupling of the strong coupling and quark masses, Comput. Phys. Commun. **133**, 43 (2000), arXiv:hep-ph/0004189.

[33] F. Herren and M. Steinhauser, Version 3 of RunDec and CRunDec, Comput. Phys. Commun. **224**, 333 (2018), arXiv:1703.03751 [hep-ph].

[34] T. R. Haar, Y. Nakamura, and H. Stüben, An update on the BQCD Hybrid Monte Carlo program, EPJ Web Conf. **175**, 14011 (2018), arXiv:1711.03836 [hep-lat].

[35] R. G. Edwards (SciDAC and LHPC Collaboration) and B. Joó (UKQCD Collaboration), The Chroma software system for lattice QCD, Nucl.Phys.Proc.Suppl. **140**, 832 (2005), arXiv:hep-lat/0409003 [hep-lat].